Carbohydrate Polymers 79 (2010) 541–546

Contents lists available at ScienceDirect

Carbohydrate Polymers

journal homepage: www.elsevier.com/locate/carbpol

Determination of the gum Arabic–chitosan interactions by Fourier Transform Infrared Spectroscopy and characterization of the microstructure and rheological features of their coacervates

Hugo Espinosa-Andrews [a,*], Ofelia Sandoval-Castilla [b], Humberto Vázquez-Torres [b], Eduardo Jaime Vernon-Carter [b], Consuelo Lobato-Calleros [c]

[a] Centro de Investigación y Asistencia en Tecnología y Diseño del Estado de Jalisco, A.C. Desarrollo y Calidad de Alimentos, Av. Normalistas 800, Guadalajara, Jalisco 44270, Mexico
[b] DF and DIPH, Universidad Autónoma Metropolitana-Iztapalapa, San Rafael Atlixco # 186, México City 09340, Mexico
[c] DPA and PCyTA, Universidad Autónoma Chapingo, Km 38.5 Carretera México-Texcoco, Texcoco 56230, Mexico

ARTICLE INFO

Article history:
Received 20 August 2009
Accepted 28 August 2009
Available online 6 September 2009

Keywords:
Complex coacervation
Potentiometric curve
FT-IR
Rheology
Microstructure

ABSTRACT

In this study gum Arabic (GA) and chitosan (Ch) electrostatic complexes were formed at different pH values (3.0, 4.5, and 6.0) and the rheological and microstructural characteristics of the coacervates were evaluated. Potentiometric titration experiments established that maximum inter-biopolymer interactions occurred at a GA–Ch weight ratio of 5:1. Fourier Transform Infrared Spectroscopy (FT-IR) results showed that the inter-biopolymeric complexes were formed through the interaction of the functional groups of both macromolecules ($-NH_3^+$ and $-COO^-$). The highest storage modulus (G') and loss modulus (G'') values were displayed by the coacervate formed at pH 4.5. Scanning electron microscopy (SEM) micrographs revealed that the coacervates were characterized by a sponge-like structure consisting of uniformly sized agglomerated interconnected particles homogeneously distributed and interspaced by heterogeneously sized vacuoles. Vacuoles size was smaller at pH 4.5 than at pH 3.0 and 6.0.

1. Introduction

Biopolymer–biopolymer interactions play an increasingly important role in modern-day researches in food science and biotechnology because they influence the microstructure formation of most biopolymer-containing systems, determining in great extent their texture, mechanical stability, consistency and, ultimately, appearance and taste (Semenova, 2007). On mixing two biopolymers in solution can display one of the three following behaviors: miscibility, thermodynamic incompatibility and complex formation. In dilute solutions, where inter-biopolymeric attractions are inhibited, the system is stable since the mixing entropy dominates and biopolymers are miscible (de Kruif & Tuinier, 2001; Tolstoguzov, 2003). Upon increased biopolymers concentration and exceeding a critical concentration, these may become partially miscible. The low entropy and the insignificant enthalpy of mixing of macromolecules are responsible of its incompatibility in a common solvent (Tolstoguzov, 2003). The forces of net repulsion between the two species in solution at the molecular level cause spontaneous separation of the system into two distinct phases. This phenomenon is known as thermodynamic incompatibility commonly exhibited in semi-dilute or concentrate solutions of biopolymers, especially when the polymers have a high molar mass (Dickinson & McClements, 1996; Walstra, 2003). The incompatibility may have various consequences; it may be a nuisance when a homogeneous liquid is desired, since it may lead to slow separation into layers. Moreover, at higher temperature the incompatibility of protein and polysaccharides is generally greater, and the lower viscosity allows faster separation to occur. On the other hand, the phenomenon can be useful in concentrating one of the polymers (Walstra, 2003).

Attractive interactions between two biopolymers can become evident in various ways: (i) formation of small soluble complex, manifesting itself in murky solutions, (ii) formation of a homogeneous weak gel, if interactions are weak, and (iii) precipitation of both biopolymers, if interactions are strong (Walstra, 2003). In the latter case, the mutual neutralization of chains bearing opposite charges decreases the net charge and hydrophilicity of forming junction zones, and promotes a compact conformation of the complex with the junction zones hidden within its hydrophobic interior. The charges neutralization of an anionic polysaccharide can

* Corresponding author. Address: Centro de Investigación y Asistencia en Tecnología y Diseño del Estado de Jalisco, A.C. Desarrollo y Calidad de Alimentos, Av. Normalistas 800, Col. Colinas de la Normal, Guadalajara, Jalisco 44270, Mexico. Tel./fax: +52 33 3345 5200.
E-mail addresses: hespinosa@ciatej.net.mx, andrewshugo@hotmail.com (H. Espinosa-Andrews).

0144-8617/$ - see front matter © 2009 Elsevier Ltd. All rights reserved.
doi:10.1016/j.carbpol.2009.08.040

also reduce the rigidity of backbone chains due to a decrease in the repulsive interaction of like-charged groups. These intermolecular arrangements give place to a separation of the solution in two phases known as coacervate complex (de Kruif & Tuinier, 2001; Tolstoguzov, 2003). Coacervation of two polyelectrolytes occurs especially at low ionic strength, for instance below 0.2 M; at higher ionic strength, the changes are sensed at very small distances only (Walstra, 2003). de Kruif and co-workers (2004) proposed that if one of the biopolymers is a strong polyelectrolyte a precipitate is formed (elastic behavior) rather than a liquid coacervate phase (viscous behavior). Coacervates have many applications in the fields of biotechnology, pharmaceutical and food industry and its specific application will depend on their structure and rheological properties. For example, one of the main applications of complex coacervation is microencapsulation, and the wall material for the encapsulation is composed by a liquid coacervate system.

In a previous work, the formation of electrostatic complexes of gum Arabic (GA) with chitosan (Ch), as a function of the biopolymers ratio, total biopolymers concentration, pH, and ionic strength was investigated. The conditions under which inter-biopolymer complexes formed were determined by performing turbidimetric and electrophoretic mobility measurements on the equilibrium phase and by quantifying the mass of the precipitated phase using elemental analysis and HPLC (Espinosa-Andrews, Báez-González, Cruz-Sosa, & Vernon-Carter, 2007; Espinosa-Andrews et al., 2008). The aim of this paper was to obtain a more in depth understanding of the interactions occurring between gum Arabic–chitosan through Fourier Transform Infrared Spectroscopy and to characterize the microstructure and rheological features of the coacervates formed at pH values of 3.0, 4.5, and 6.0, so that with this information specific future applications of these coacervates can be achieved.

2. Materials and methods

2.1. Materials

Chitosan (Ch) (medium molecular weight, degree of deacetylation: 79%) was purchased from Sigma–Aldrich (St. Louis, MO, USA). Gum Arabic (GA) (*Acacia senegal*) tear drops were purchased from Grupo Aselac S.A de C.V. (Tezoyuca, State of México, México). Hydrochloric acid (HCl), sodium hydroxide (NaOH), ethanol (C_2H_6O), and glutaraldehyde ($C_5H_8O_2$) were purchased from J.T. Baker (Xalostoc, State of México, México).

2.2. Stock solutions

Ch (2 wt.%) and GA (10 wt.%) stock solutions were prepared by dispersing the former in MilliQ-grade water (18.2 mΩ) with 0.1 N HCl and the latter in MilliQ-grade water. The solutions were gently stirred for 12 h and stored overnight at 4 °C to ensure complete hydration of the biopolymers.

2.3. Equivalence point of biopolymers solutions

The equivalence point of polysaccharide stock solutions (2 wt.% Ch and 10 wt.% GA) was determined from the potentiometric titration curves, which was continuously stirred. Titrations were carried out with aliquots of 0.5 mL of NaOH 0.1 N. The precise concentration of base was obtained by titrating with a standard 0.01 N HCl solution. A 60 s time lag was allowed between two doses to ensure that the reaction has reached equilibrium. The resulting pH values were recorded using a Vernier pH-BTA (Beaverton, OR, USA) at 25 °C.

2.4. Coacervate preparation

GA–Ch coacervate was prepared by blending the two polysaccharides solutions in the needed proportions, estimated on basis of the value of the equivalence point between them, which allowed the charge neutralization of the functional groups. The pH values (3.0, 4.5, and 6.0) of the solutions were adjusted by adding either HCl (0.1 N) or NaOH (0.1 N). The mixed solutions were left to stand at room temperature (20 ± 2 °C) for 72 h to allow the phases equilibrium. Afterwards the coacervate phase was separated by decantation.

2.5. Fourier Transform Infrared Spectroscopy (FT-IR)

Stock solutions of GA, Ch, and GA–Ch coacervate (pH of 4.5) were dried at 45 °C until constant weight in a vacuum dryer. FT-IR spectra of solid samples of GA, Ch, and GA–Ch coacervate were obtained by using a spectrophotometer FT-IR GX System (Perkin–Elmer, Shelton, CT, USA) coupled to an ATR *DuraSample II* accessory. All the spectra were an average of 16 scans from 4000 to 650 cm^{-1} at a resolution of 2 cm^{-1}.

2.6. Rheological measurements

Viscoelastic properties of the coacervates were measured with a MCR 300 rheometer (Paar Physica, Messtechnik, Stuttgart, Germany) at 25 °C. Truncated cone–plate geometry (1°, 75 mm diameter) was used, in which the truncated cone had a gap of 0.05 mm between the flat surfaces of both elements. The samples were put into a humidity trap to avoid evaporation of the solvent. Afterwards, oscillatory single frequency time sweep curves were carried out at constant angular frequency and strain deformation of 10 rad s^{-1} and 1%, respectively, until constant elastic modulus (G') was achieved. Each sample had a characteristic time to achieve constant G', and samples were left to stand after their loading into the rheometer for this period of time to allow their structure recovery. The amplitude strain (0.01–100%) sweeps were determined at an angular frequency (ω) of 10 rad s^{-1} in order to determine the linear viscoelastic region, i.e., the curve region where the dynamic storage modulus (G') and loss modulus (G'') are independent of strain. The oscillating sweep measurements were carried out over an extended angular frequency (ω) domain of 100–0.1 rad s^{-1}.

2.7. Relative density of coacervate phase

Relative density of the coacervates was measured with a digital densimeter DMA35 (Anton Paar, Graz, Austria) at 25 °C. The instrument provided the density of the sample at the temperature of measure relative to the water density at 20 °C.

2.8. Scanning electron microscopy (SEM)

Coacervates samples were fixed in 2 wt.% glutaraldehyde solution for 90 min, dehydrated in increasing concentrations of ethanol aqueous solutions (50%, 60%, 70%, 80%, 90%, and 100%, 30 min in each) and placed in acetone for 1 h. Samples were critical point dried in CPA II Technics Critical Point Dryer (Tousimis, Rockville, MD, USA). Each sample was fragmented and was mounted on stubs with the fractured face uppermost, and coated with a thin layer of gold in a Fine Coat Ion Sputter JFC 1100 (Jeol Ltd., Akishima, Japan) (Lobato-Calleros, Rodríguez, Sandoval-Castilla, Vernon-Carter, & Alvarez Ramirez, 2006). A high vacuum JEOL Scanning Electron Microscope JMS-6360LY (Jeol Ltd., Akishima, Japan), was used at 20 kV to obtain the SEM image for each sample at a magnification of 5000×. Selected micrographs are presented.

2.9. Statistical analysis

All the measurements were done by triplicate, and their means were reported. Statistical analysis was done through the program Statistica 8.0. To determine the statistically significant difference between values were done with an analysis of variance one-way and Tukey HSD test. Differences were considered statistically significant ($p < 0.05$).

3. Results and discussion

3.1. Equivalence point

The equivalence point of biopolymers solutions was determined by the inflexion point from the titrations curves of the biopolymers stocks solutions (Fig. 1). When NaOH is titrated into the biopolymer solution, it dissociates completely and produces sodium cations and hydroxide anions, and the COO^- and $—NH_3^+$ groups are neutralized by the sodium cations and hydroxide anion, respectively. Both Ch (2 wt.%) and GA (10 wt.%) stocks solutions had 0.25 milliequivalents of NaOH.

Fig. 2 shows the ratio of milliequivalents of GA/Ch as a function of the biopolymers initial ratio ($R_{GA/Ch}$). When both polysaccharides are mixed in a ratio where their opposite charges present the same magnitude, the attraction force between both polysaccharides is maximized and an intense interaction takes place. At this point, the ionized groups of both macromolecules are mutually neutralized leading the formation of insoluble complexes (complex coacervation). The maximum coacervation (in terms of coacervate yield) occurs at the equivalent mixing ratio of polysaccharides (1:1) corresponding to 5 g of GA per gram of Ch. These results are in agreement with the results reported by Espinosa-Andrews and co-workers (2007) who found a stoichiometric charge ratio of 5:1 (GA:Ch) by turbidimetric, electrophoretic mobility, and coacervate yield measurements.

3.2. Fourier Transform Infrared Spectroscopy

The GA, Ch, and GA–Ch coacervate FT-IR spectra (Fig. 3) were analyzed in their solid state in order to be unaffected by the strong water absorption, in particular in the amide I band region (1720–1580 cm^{-1}) characteristic of vibrations of peptidic bonds (Renard, Lavenant-Gourgeon, Ralet, & Sanchez, 2006). The FT-IR spectrum of Ch showed a typical band at 3230 cm^{-1} concerned with —OH groups. This band is broad because it overlaps the stretching band of —NH. Other bands were also observed: at 2925 cm^{-1} corresponding to stretching vibration of C—H bond; at 1635 cm^{-1} a

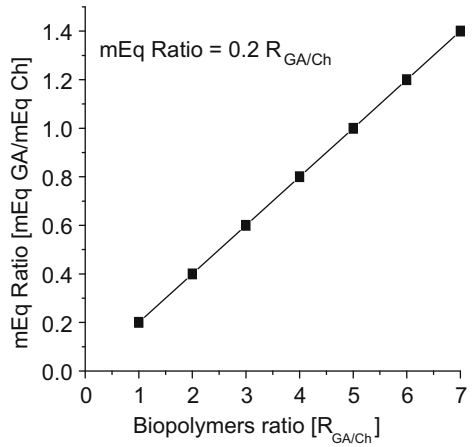

Fig. 2. Gum Arabic/chitosan milliequivalent ratio as a function of gum Arabic/chitosan biopolymers ratio.

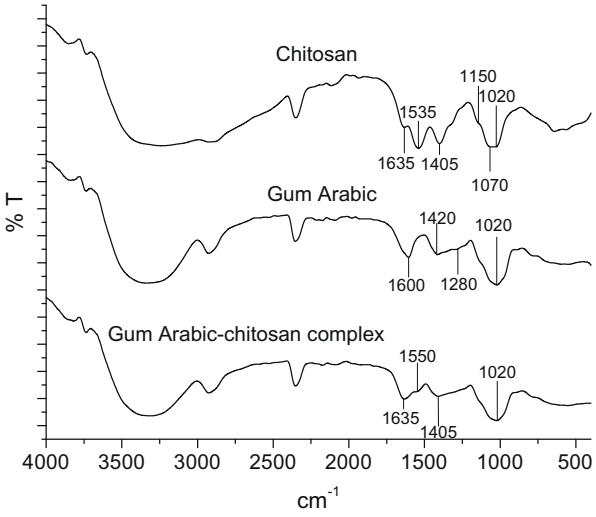

Fig. 3. FT-IR spectra of gum Arabic and chitosan at blank, and gum Arabic–chitosan coacervate (GA–Ch).

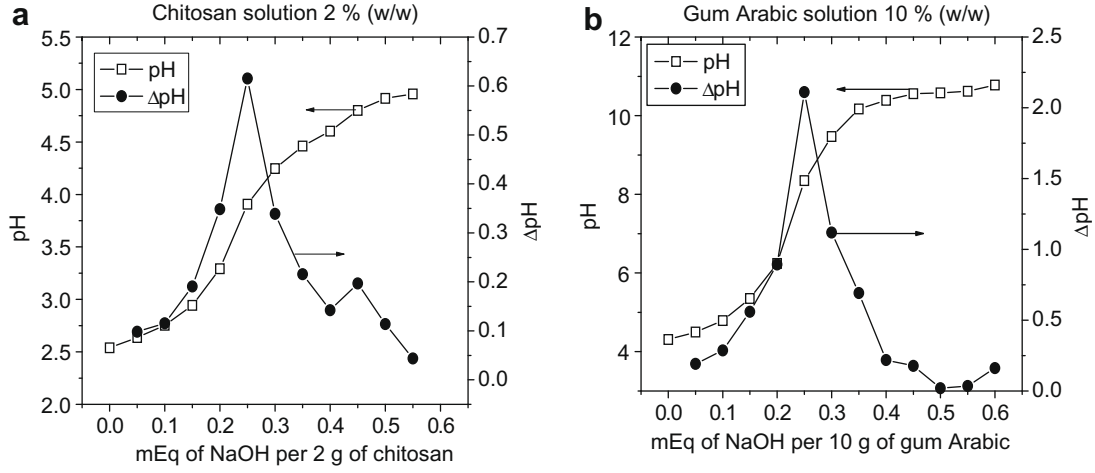

Fig. 1. (a) milliequivalent of NaOH per 2 g of chitosan; (b) milliequivalent of NaOH per 10 g of gum Arabic.

characteristic amide I band attributed to C=O vibration of the acetylated units (—$CONH_2$ groups); and at 1535 cm^{-1} a strong band associated to the amide III (—NH_3^+ groups) (Grant, Cho, & Allen, 2006). The peak at 1405 cm^{-1} was the joint contribution of the vibration of —OH and —CH (Qian, Cui, Ding, Tang, & Yin, 2006). The band at 1150 cm^{-1} corresponds to the symmetric stretching of C—O—C; bands at 1070 cm^{-1} and 1020 cm^{-1} are associated to the C—O stretching vibration (de Vasconcelos et al., 2006). GA showed typical bands of the —OH bond at 3330 cm^{-1}. Two strong bands at 1600 cm^{-1} and 1420 cm^{-1} are due to asymmetric and symmetric stretching vibration of the carboxylic acid salt —COO^- and bands at 1280 cm^{-1} and 1020 cm^{-1} due to the stretching of the C—O bond (Colthup, Daly, & Wiberley, 1990). GA–Ch complexes showed a band at 3295 cm^{-1} attributed to —NH_2 and —OH groups stretching vibration. As a result of the interaction of the biopolymers, the FT-IR of the GA–Ch coacervate changed significantly in the carbonyl-amide region. The —NH_3^+ groups (band at 1535 cm^{-1}) and asymmetric and symmetric —COO^- stretching vibration at 1600 cm^{-1} and 1420 cm^{-1}, respectively, disappeared, indicating the electrostatic interaction between the amine groups of Ch (—NH_3^+) and carboxyl groups of GA (—COO^-).

3.3. Rheological measurements

The results obtained from the frequency time sweep curves provided the characteristic times required for the coacervates to achieve structure recovery after sample loading. In general terms, all the coacervates, independently of their pH took about 40 min to reach a constant G′ value (data not shown). With basis on these experiments, a delayed time of 50 min was set for the subsequent rheological measurements. The amplitude strain sweep curves indicated that the point of critical strain (limit of the linear viscoelastic region, where the rheological properties are not strain dependent) occurred under a strain of 5% (data not shown) for all the samples. With basis on these results, a constant strain of 1% was chosen to carry out the frequency sweeps. Fig. 4 shows the frequency sweeps curves of GA–Ch coacervates at different pH values, where the viscoelastic nature of the coacervates can be appreciated. All the coacervates exhibited a predominantly liquid viscoelastic behavior since the loss modulus (G″) was higher than storage modulus (G′) over the whole frequency range studied. Fig. 4 shows that the GA–Ch complex (at different pH) behaved like typical polymer systems in which there is not gel formation, but a cross-linked network probably with the cross-over point (G′ = G″) at high frequencies (≈100 rad/s). The tan δ decreased moderately with increasing frequency without being 1 (data not shown). This behavior confirms the presence of a cross-linked network, with higher viscoelastic characteristics at pH 4.5 than at pH 6.0 and 3.0. The viscoelastic property of the GA–Ch complex at pH 4.5 was significantly higher than those of the coacervates formed at pH 3.0 and 6.0, showing the follow order: 4.5 > 6.0 > 3.0. A predominantly viscous behavior has been reported for other coacervates: agar–gelatin (Singh, Aswal, & Bohidar, 2007), bovine serum albumin (BSA)–poly-diallyldimethylammonium chloride (PDADMAC) (Bohidar, Dubin, Majhi, Tribet, & Jaeger, 2005; Kayitmazer, Strand, Tribet, Jaeger, & Dubin, 2007), and whey protein–gum Arabic coacervates (Weinbreck, Wientjes, Nieuwenhuijse, Robijn, & de Kruif, 2004). In the latter, the G″ values were approximately ten times higher than the G′ values at a pH of 4.0. On the other hand, chitosan–BSA coacervates were characterized by a cross-over between G″ and G′ at ω 10 s^{-1} (Kayitmazer et al., 2007).

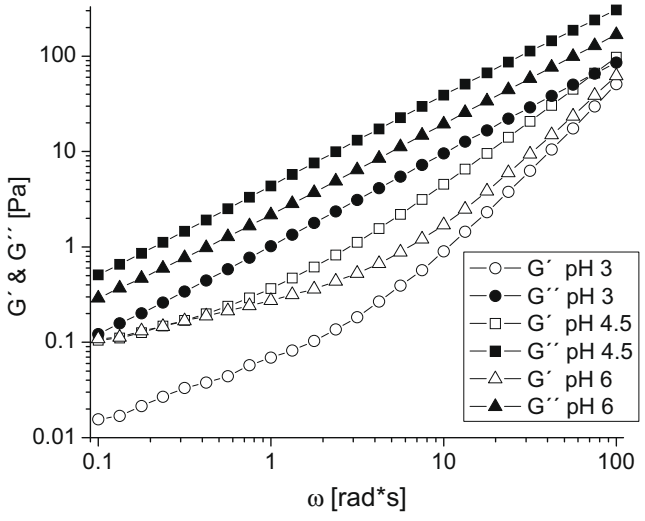

Fig. 4. Frequency sweeps of the gum Arabic–chitosan coacervates at different pH values (3.0, 4.5, and 6.0) at 25 °C.

As the pH moves away from a value of 4.5 the charge balance due to the ionization degree between both macromolecules drifts away from its stoichiometric ratio, causing a decrease in coacervate yield and, eventually, the appearance of soluble complexes. A variation in pH resulted in a change of the net charge of the biopolymers causing conformational changes in their backbones, reducing the sites available for moieties interaction (weak interparticle interaction). Both, the net charge of biopolymers and the stoichiometry of their electrostatic complexes are affected by changes of pH values. When the pH decreases, the insoluble complexes are enriched with the anionic polysaccharide (Tolstoguzov, 2003). Changes in the electrostatic composition could explain the observed variation in the networks relative density (see below) and the viscoelastic behavior with pH variation.

3.4. Scanning electron microscopy

Scanning electron microscopy (SEM) micrographs revealed that all the GA–Ch coacervates displayed a sponge-like microstructure, where well-connected small size agglomerated particles and homogeneously distributed formed the structural matrix, which was interspaced by heterogeneously sized vacuoles. Vacuoles sizes were smaller at pH 4.5 than at pH 3.0 or 6.0, thus pH strongly influenced the microstructural features of the coacervates (Fig. 5). Vacuoles apparent diameters ranged from 0.47–2.99, 0.18–1.45, and 0.24–2.46 μm for pH values of 3.0, 4.5, and 6.0, respectively.

Schmitt and co-workers (2001) observed that the structure of β-lactoglobulin–Acacia coacervates using confocal scanning laser microscopy were characterized by spherical vesicular structures (foam-like) whose apparent diameter ranged approximately from 1 to 4 μm. When two macromolecules with opposing charges interact associatively they give rise to the formation of macromolecular networks (complex coacervation), trapping water molecules (vacuoles) within the network, and the water in the coacervate phase contributes to the complex structure (Burgess, 1990).

A highly cross-linked compact network resulted in a structure displaying a relatively lower number of vacuoles, and a high relative density GA–Ch coacervate. Thus, the relative density of the coacervate formed at pH 4.5 (1.100 ± 0.005) was significantly higher than those of the coacervates formed at pH 3.0 (1.075 ± 0.005) and 6.0 (1.065 ± 0.005). Tan and coworkers (2005) observed that microgels of methacrylic acidethyl acrylate cross-linked with di-allyl phthalate exhibited relative lower swelling when cross-linked density increased.

In this work, a close interrelationship existed between the density of the coacervate network structure and their viscoelastic re-

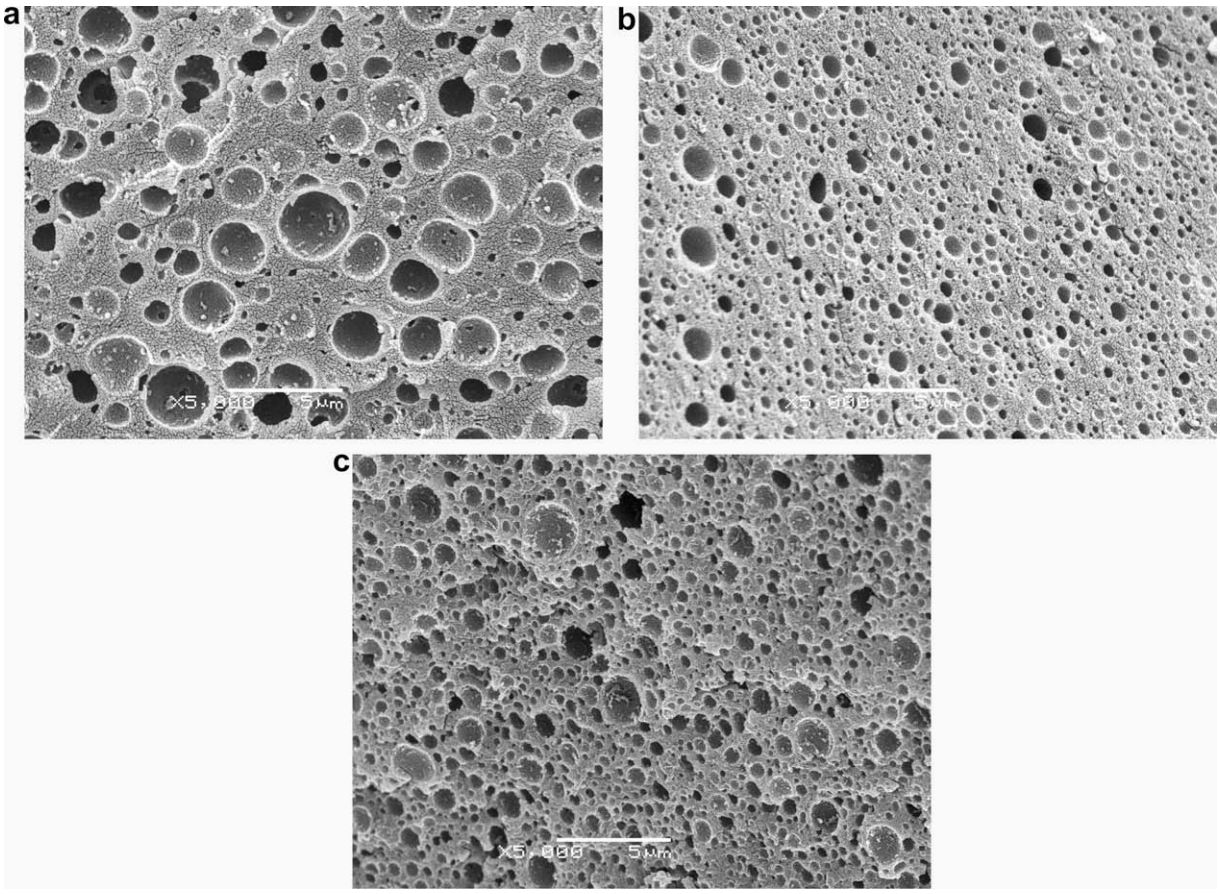

Fig. 5. SEM micrographs of gum Arabic–chitosan coacervates at: (a) pH 3.0, (b) pH 4.5, and (c) pH 6.0.

sponse. The higher the relative density of the network structure, the higher its viscoelastic moduli values.

4. Conclusions

The potentiometric titration of biopolymers solutions is a quick method for establishing the relative biopolymers concentration required to form an electrostatic complex. Our results showed that the gum Arabic–chitosan coacervate formation took place when these biopolymers were mixed in a 5:1 ratio. The FT-IR results confirmed that the complex was formed through the electrostatic interaction between the amine groups of chitosan ($—NH_3^+$) and carboxyl groups of gum Arabic ($—COO^-$). The rheological behavior of coacervates had a predominantly liquid viscoelastic character independently of the pH at which they were formed. The highest viscoelastic moduli values were exhibited by the coacervate formed at pH 4.5. The coacervates were characterized by a sponge-like microstructure, which was affected also by variation of pH. At pH 4.5 the coacervate microstructure had the highest relative density and the smallest vacuoles in comparison to the coacervates obtained at pH 3.0 and 6.0.

This study provides important insights for designing tailor made complexes for improving the functional properties of specific foods.

Acknowledgment

We would like to thank the Consejo Nacional de Ciencia y Tecnología de México (CONACyT) for partially financing this study through Grant U81157-Z and the Biol. Yolanda Hornelas-Uribe of the Instituto de Ciencias del Mar y Limnología of the Universidad Nacional Autónoma de México for the expertise provided for obtaining the SEM micrographs.

Reference

Bohidar, H., Dubin, P. L., Majhi, P. R., Tribet, C., & Jaeger, W. (2005). Effect of protein–polyelectrolyte affinity and polyelectrolyte molecular weight on dynamic properties of bovine serum albumin–poly(diallyldimethylammonium chloride) coacervates. *Biomacromolecules, 6*, 1573–1585.

Burgess, D. J. (1990). Practical analysis of complex coacervate systems. *Journal of Colloid and Interface Science, 140*, 227–238.

Colthup, N. B., Daly, L. H., & Wiberley, S. E. (1990). *Introduction to infrared and Raman spectroscopy* (3rd ed., p. 319). San Diego, CA.: Academic Press, Inc.

de Kruif, C. G., & Tuinier, R. (2001). Polysaccharide protein interactions. *Food Hydrocolloid, 15*, 555–563.

de Kruif, C. G., Weinbreck, F., & de Vries, R. (2004). Complex coacervation of proteins and anionic polysaccharides. *Current Opinion in Colloid & Interface Science, 9*, 340–349.

de Vasconcelos, C. L., Bezerril, P. M., dos Santos, D. E., Dantas, T. N., Pereira, M. R., & Fonseca, J. L. (2006). Effect of molecular weight and ionic strength on the formation of polyelectrolyte complexes based on poly(methacrylic acid) and chitosan. *Biomacromolecules, 7*, 1245–1252.

Dickinson, E., & McClements, D. J. (1996). *Advances in food colloids* (pp. 5–10). London: Blackie Academic & Professional.

Espinosa-Andrews, H., Báez-González, J. G., Cruz-Sosa, F., & Vernon-Carter, E. J. (2007). Gum Arabic–chitosan complex coacervation. *Biomacromolecules, 8*(4), 1313–1318.

Espinosa-Andrews, H., Lobato-Calleros, C., Loeza-Corte, J. M., Beristain, C. I., Rodríguez-Huezo, M. E., & Vernon-Carter, E. J. (2008). Quantification of the composition of gum arabic–chitosan coacervates by HPLC. *Revista Mexicana de Ingeniería Química, 7*(3), 293–298.

Grant, J., Cho, J., & Allen, C. (2006). Self-assembly and physicochemical and rheological properties of a polysaccharide–surfactant system formed from the cationic biopolymer chitosan and nonionic sorbitan esters. *Langmuir, 22*, 4327–4335.

Kayitmazer, A. B., Strand, S. P., Tribet, C., Jaeger, W., & Dubin, P. L. (2007). Effect of polyelectrolyte structure on protein-polyelectrolyte coacervates: Coacervates of

bovine serum albumin with poly(diallyldimethylammonium chloride) versus chitosan. *Biomacromolecules, 8*, 3568–3577.

Lobato-Calleros, C., Rodríguez, E., Sandoval-Castilla, O., Vernon-Carter, E. J., & Alvarez Ramirez, J. (2006). Reduced-fat white fresh cheese-like products obtained from W1/O/W2 multiple emulsions: Viscoelastic and high-resolution image analyses. *Food Research International, 39*, 678–685.

Qian, F., Cui, F., Ding, J., Tang, C., & Yin, C. (2006). Chitosan graft copolymer nanoparticles for oral protein drug delivery: Preparation and characterization. *Biomacromolecules, 7*, 2722–2727.

Renard, D., Lavenant-Gourgeon, L., Ralet, M. C., & Sanchez, C. (2006). *Acacia senegal* gum: Continuum of molecular species differing by their protein to sugar ratio, molecular weight, and charges. *Biomacromolecules, 7*, 2637–2649.

Schmitt, C., Sanchez, C., Lamprecht, A., Renard, D., Lehr, C. M., de Kruif, C. G., et al. (2001). Study of β-lactoglobulin: Acacia gum complex coacervation by diffusing-wave spectroscopy and confocal scanning laser microscopy. *Colloids and Surfaces B: Biointerfaces, 20*, 267–280.

Semenova, M. G. (2007). Thermodynamic analysis of the impact of molecular interactions on the functionality of food biopolymers in solution and in colloidal systems. *Food Hydrocolloid, 21*, 23–45.

Singh, S., Aswal, V. K., & Bohidar, H. B. (2007). Structural studies of agar–gelatin complex coacervates by small angle neutron scattering, rheology and differential scanning calorimetry. *International Journal of Biological Macromolecules, 41*, 301–307.

Tan, B. H., Tam, K. C., Yee, T., Lam, C., & Tan, C. B. (2005). Microstructure and rheology of stimuli-responsive microgel systems—effect of cross-linked density. *Advances in Colloid and Interface Science, 113*(2–3), 111–120.

Tolstoguzov, V. B. (2003). Some thermodynamic considerations in food formulation. *Food Hydrocolloid, 17*, 1–23.

Walstra, P. (2003). *Physical chemistry of foods* (pp. 179–187). New York-Basel: Marcel Dekker, Inc.

Weinbreck, F., Wientjes, R. H. W., Nieuwenhuijse, H., Robijn, G. W., & de Kruif, C. G. (2004). Rheological properties of whey protein/gum arabic coacervates. *Journal of Rheology, 48*(6), 1215–1228.